Putative Identification of 12 Isomeric and 21 Non-isomeric Compounds from Leaves of Rubus Alceifolius Poir Using Database-affinity UHPLC-Q-Exactive-Qrbitrap-MS/MS

xican Li (lixican@126.com)
Guangzhou University of Chinese Medicine https://orcid.org/0000-0002-4358-3993
Jingyuan Zeng
Guangzhou University of Chinese Medicine
Rongxin Ca
Guangzhou University of Chinese Medicine
Shaoman Chen
Guangzhou University of Chinese Medicine
Chunhou Li
Guangzhou University of Chinese Medicine
Nana Jin
Guangzhou University of Chinese Medicine
Tingshan Chen
Guangzhou University of Chinese Medicine
Xiaohua Lin
Guangzhou University of Chinese Medicine
Sunbal Khan
University of Malakand

Research Article

Keywords: Rubus Alceifolius leaf, isomers recognition, caffeoylquinic acid, UPLC-Q- Orbitrap-MS

Posted Date: November 14th, 2023

DOI: https://doi.org/10.21203/rs.3.rs-3450438/v1

Abstract

This is the first article to report of the chemical profile of the leaves of *Rubus alceifolius* Poir, a widely distributed medicinal plant in the Eastern Hemisphere. Fresh leaves of *R. alceifolius* were treated by a set of experimental protocols to prepare a lyophilized aqueous extract. A novel strategy was used to analyze the extract, i.e., The extract was then analyzed using a new strategy, i.e., database-affinity ultra-high-performance liquid chromatography-quadrupole-Exactive-Orbitrap-tandem mass spectrometry (UHPLC-Q-Exactive-Orbitrap-MS/MS). Using MS/MS at full elucidation and comparison with the database, 33 compounds were putatively identified, including 12 flavonoid derivatives, 6 phenolic acid derivatives, 6 caffeoylquinic acids, two tea polyphenols, and others. Especially, 12 isomers have been strictly distinguished, including apigenin *vs* 2'-hydroxydaidzein, luteolin 7-O-glucuronide *vs* scutellarin, (+) catechin *vs* (-) epicatechin, 3-*O*-caffeoylquinic acid *vs* 4-*O*-caffeoylquinic acid *vs* 5-*O*-caffeoylquinic acid, and 3,4-*O*-dicaffeoylquinic acid *vs* 3,5-*O*-dicaffeoylquinic acid *vs* 4,5-*O*-dicaffeoylquinic acid. In addition, 21 non-isomeric compounds were also found under both negative and positive ion models, such as ellagic acid and gallic acid. Structural comparison suggested that there were biogenetic relationships among the flavonoid derivatives, such as glycosidation and hydroxylation. All these new findings will help to understand the substance basis of the traditional medicinal functions of *R. Alceifolius*. The structural comparison suggested biogenetic relationships between flavonoid derivatives, such as glycosidation and hydroxylation. These findings will allow the scientific community to better understand *R. Alceifolius* traditional medicinal functions.

1. Introduction

Rubus alceifolius Poir, is a plant belonging to the Rosaceae family. It is native to the Eastern Hemisphere including Assam, Borneo, Cambodia, China, East Himalaya, Jawa, Laos, Lesser Sunda Island, Malaya, Myanmar, Sulawesi, Sumatera, Taiwan, Thailand, and Vietnam. However, it has been recently introduced by humans also introduced into other areas, such as including Burundi, Comoros, Mauritius, Queensland, and Réunion [1], [2].

The genus Rubus is traditionally used as a medicinal plant around the world by native communities.[3, 4] The leaves of *R. alceifolius* however have a sweet and plain flavor taste. According to the traditional Chinese medicine (TCM), they can also be used as a traditional medicine for treatment of diuresis, detoxification, and bruise healing also broadly used to treat various types of hepatitis in China [5]. In accordance with the Clarivate database, no chemical studies regarding *R. alceifolius* leaves have been reported yet [6].

Our team however established a database-affinity UHPLC-Q-Exactive-Orbitrap-MS/MS putative identification strategy [7, 8]. This strategy could completely elucidate the MS fragment, and definitely give stereo-configuration of chiral compounds, as well as clearly discriminate the isomers [9]. Through the strategy, we tried to accomplish the task of determining the chemical profile of *R. alceifolius* leaves. This would facilitate to understanding the substance basis of the traditional function of *R. alceifolius* leaves and to develop them a natural drug or bio-resource. Considering the wide distribution and high fertility of *R. alceifolius* [2], the development of its leaves will promise a broad prospect.

2. Materials and Methods

2.1 Plant materials and chemicals

The mature leaves of "*Rubus alceifolius* Poir" were clipped in the Guangdong Province Traditional Chinese Medicine Resource Preservation Garden for 4th National Survey of Traditional Chinese Medicine Resources. The preservation garden locates at Yaowang Hill in Guangzhou University of Chinese Medicine (23.039° north latitude, 113.388° east longitude, altitude 20 m, Guangzhou, China). The clipped leaves were collected on July 12, 2023 (Fig. 1). Prior to *R. alceifolius* analysis the leaves were identified with standard literature key. Methanol and water, purchased from Merck Sigma-Aldrich (Shanghai, China), both for sample solution preparation and apparatus analysis were of mass spectra purity.

2.2 Authentic standards

D-gluconic acid (Cas. 526-95-4, $C_6H_{12}O_7$, M.W. 196.155, 98%) and (+)-catechin (Cas. 154-23-4, $C_{15}H_{14}O_6$, M.W. 290.27, 98%) were from Merck-Sigma Co., Ltd. (Shanghai, China). Quinic acid (Cas. 77-95-2, $C_7H_{12}O_6$, M.W. 192.16, 98%), methyl gallate (Cas. 99-24-1, $C_8H_8O_5$, M.W. 192.16, 98%), and 5-hydroxymethylfurfural (Cas. 67-47-0, $C_6H_6O_3$, M.W. 126.111, 98%) were obtained from Herbest Biotech Co., Ltd (Baoji, China). Viscidulin I (Cas. 92519-95-4, $C_{15}H_{10}O_7$, M.W. 302.24, 98%) was obtained BioBioPha Co., Ltd. (Kunming, China). Chlorogenic acid (Cas. 327-97-9, $C_{16}H_{18}O_9$, M.W. 354.31, 98%), epicatechin (Cas. 490-46-0, $C_{15}H_{14}O_6$, M.W. 290.27, 97%), and tiliroside (Cas. 20316-62-5, $C_{30}H_{26}O_{13}$, M.W. 594.52, 98%) were from Sichuan Weikeqi Biological Technology Co., Ltd. (Chengdu, China). Caffeic acid (Cas. 331-39-5, $C_9H_8O_4$, M.W. 180.16, 98%), *cis*-4-hydroxycinnamic acid (Cas. 501-98-4, $C_9H_8O_3$, M.W. 164.16, 98%), isochlorogenic acid B (3,4-dicaffeoylquinic acid, Cas. 14534-61-3, $C_{25}H_{24}O_{12}$, M.W. 516.45, 98%), luteolin 7-*O*-glucuronide (Cas. 29741-10-4, $C_{21}H_{18}O_{12}$, M.W. 462.36, 97%), ellagic acid (Cas. 476-66-4, $C_{14}H_6O_8$, M.W. 302.28, 98%), isoquercitrin (Cas. 482-35-9, $C_{21}H_{20}O_{12}$, M.W. 464.38, 98%), isochlorogenic acid C (Cas. 57378-72-0, $C_{25}H_{24}O_{12}$, M.W. 516.45, 98%), baicalin (Cas. 21967-41-9, $C_{21}H_{18}O_{11}$, M.W. 446.37, 97%), 2'-hydroxydaidzein (Cas. 7678-85-5, $C_{15}H_{10}O_5$, M.W. 270.24, 98%), scutellarin (Cas. 27740-01-8,

$C_{21}H_{18}O_{12}$, M.W. 462.37, 98%), cosmosiin (Cas. 578-74-5, $C_{21}H_{20}O_{10}$, M.W. 432.38, 98%), isochlorogenic acid A (Cas. 2450-53-5, $C_{25}H_{24}O_{12}$, M.W. 516.45, 97%), astragalin (kaempferol 3-*O*-glucoside, Cas. 480-10-4, $C_{21}H_{20}O_{11}$, 448.38, 97%), apigenin (Cas. 520-36-5, $C_{15}H_{10}O_5$, M.W. 270.24, 98%), 6-gingerol (Cas. 23513-14-6, $C_{17}H_{26}O_4$, M.W. 294.39, 98%), kaempferol (Cas. 520-18-3, $C_{15}H_{10}O_6$, M.W. 286.24, 98%), and ferulic acid (Cas. 1135-24-6, $C_{10}H_{10}O_4$, M.W. 194.184, 98%) were obtained from Chengdu Alfa Biotech. Ltd. (Chengdu, China). Cryptochlorogenic acid (Cas.905-99-7, $C_{16}H_{18}O_9$, M.W. 354.311, 97%), quercetin 3-O-β-D-glucuronide (Cas. 22688-79-5, $C_{21}H_{18}O_{13}$, M.W. 478.36, 97%), 5-caffeoylquinic acid (Cas. 906-33-2, $C_{16}H_{18}O_9$, M.W. 354.309, 98%), gallic acid (Cas. 149–91 – 7, $C_7H_6O_5$, M.W. 170.1, 99%) were obtained from Biopurify Phytochemicals, Ltd. (Chengdu, China). Betaine (Cas. 107-43-7, $C_5H_{11}NO_2$, M.W. 117.148, 98%) was from Shanghai Yuanye Biotechnology Co., Ltd. (Shanghai, China). Ethyl stearate (Cas. 111-61-5, $C_{20}H_{40}O_2$, M.W. 312.53, 98%) and (+)-4-cholesten-3-one (Cas. 601-57-0, $C2_7H_{44}O$, M.W. 384.638, 98%) were from TCI Chemical Co. (Shanghai, China).

2.3 Preparation of sample solution and authentic standard solution

2.3.1 Preparation of lyophilized aqueous extract and corresponding sample solution

To avoid the possible insoluble impurity and solvent effect [10], *R. alceifolius* leaves were extracted using distilled water. The extraction process mainly included mashing, soaking, boiling, filtering, and lyophilizing steps. The design of these steps was consulted with the previous report [11] and intuitively described as Fig. 2. Thereafter, a brown lyophilized powder was obtained, which was then re-dissolved using 80% methanol at 30 mg/mL. The methanolic solution was then re-filtered using a 0.45 μm organic filter membrane, to afford a sample solution. For further analysis, the sample solution was stored at 2–6 ℃.

2.3.2 Preparation of authentic standard solution

All authentic standards listed in Section 2.2 were dissolved in methanol at a concentration of 30 μg/mL, respectively. Each solution was transferred into a flask and subsequently filtered through a 0.45 μm membrane. Afterwards, the filtrate was stored at 2–6 ℃for further analysis [12].

2.4 Putative identification using software and MS spectra elucidation

The main operations regarding injection, data acquisition, and analysis were controlled by the Xcalibur 4.1 package (Thermo Fisher Scientific Inc., Waltham, MA, USA). The package mainly included a TraceFinder General Quan software, a *m/z*Vault software, and a FreeStyle viewing software. These were equipped in the UHPLC-Q-Exactive Orbitrap-MS apparatus. Before data acquisition, the background sign was zeroed using a blank solvent. The acquired data were then exported to TraceFinder General Quan for *m/z* extraction, to afford corresponding MS spectra [13].

Among the main parameters are mass range: 100–1500 Da; mass tolerance: 5 ppm; S/N threshold: 5; isotopic pattern fit threshold: 90%. Xcalibur 4.1 was used to screen the MS spectra and corresponding top 5 secondary spectra. By comparing with authentic standards in four parameters (retention time, molecular ion peak, MS/MS profile, and characteristic fragments), the compounds were preliminary nominated by TraceFinder and putatively identified by manual [14].

3. Results

3.1 Putative identification based on database-affinity UHPLC-Q-Exactive-Orbitrap-MS analysis

3.1.1 Main experimental results of all identified compounds

3.1.2 TIC diagrams under negative model and positive model

3.1.3 Collection of structures of all identified compounds

3.1.4 Typical MS/MS spectra and fragmenting pathway elucidation

4. Discussion

A negative ion model indicated that *R. alceifolius* leaves extract enriched 30 compounds. In addition, three compounds were also found under the positive ion model. Thus, the study has putatively identified 33 compounds in total, by means of the database-affinity UHPLC-Q-Exactive-Orbitrap-MS/MS strategy. From the angle of nominal level values, ellagic acid and gallic acid showed the highest abundance (Table 1 and Figs. 3–4).

Table 1
The main experimental results of 33 putatively identified compounds (**1–33**)

No.	RT min	Name	Molecular ion	Observed *m/z* value	Theoretical *m/z* value	Error (δ ppm)	Nominal level	Characteristic MS/MS fragment peak *m/z*	Bioactive effect
1	0.52	quinic acid	$C_7H_{11}O_6^-$	191.0553	191.0561	4.1872	1.87×10^7	173.0450, 155.0344, 127.0395	No report
2	0.55	D-gluconic acid	$C_6H_{11}O_7^-$	195.0503	195.051	3.5888	1.09×10^5	177.0395, 159.0288, 129.0185	No report
3	0.57	betaine	$C_5H_{12}NO_2$	118.0863	118.0863	0	1.03×10^6	74.0609, 58.0659	neuroprotection [15]
4	0.84	gallic acid	$C_7H_5O_5^-$	169.0133	169.0142	5.3250	2.59×10^7	125.0239, 107.0133	antioxidant [16]
5	1.18	5-hydroxymethylfurfural	$C_6H_7O_3$	127.0389	127.039	0.7872	1.15×10^6	109.0290, 81.0340	No report
6	1.81	5-caffeoylquinic acid	$C_{16}H_{17}O_9^-$	353.088	353.0878	0.5664	6.86×10^5	191.0553, 179.0339, 173.0439, 135.0442	antioxidant, anti-inflammation [17]
7	2.82	(+)-catechin	$C_{15}H_{13}O_6^-$	289.072	289.0718	0.6919	6.63×10^4	245.0814, 203.0708, 151.0395, 109.0290	antioxidant [18]
8	3.03	methyl gallate	$C_8H_7O_5^-$	183.0292	183.0299	3.8245	3.81×10^5	168.0059, 140.0110, 124.0160, 111.0082	anti-tumor, anti-inflammatory, antioxidant [19]
9	4.17	chlorogenic acid	$C_{16}H_{17}O_9^-$	353.0878	353.0878	0.0000	2.68×10^6	191.0554, 173.0446, 161.0239, 109.0283	antioxidant[20] cytoprotection [21]
10	4.43	caffeic acid	$C_9H_7O_4^-$	179.0341	179.035	5.0269	1.80×10^6	135.0446, 117.0340	antioxidant [22]
11	4.98	cryptochlorogenic acid	$C_{16}H_{17}O_9^-$	353.0881	353.0878	0.8496	6.04×10^5	191.0556, 173.0447, 161.0235, 135.0446	anti-inflammation [23]
12	7.25	(-) epicatechin	$C_{15}H_{13}O_6^-$	289.0716	289.0718	0.6919	3.82×10^5	245.0813, 221.0809, 203.0708	antioxidant [24]
13	7.77	*cis*-4-hydroxycinnamic acid	$C_9H_7O_3^-$	163.0393	163.0401	4.9068	3.27×10^5	119.0493, 117.0337, 93.0335	antioxidant [25]
14	8.73	ferulic acid	$C_{10}H_9O_4^-$	193.0499	193.0506	3.6260	1.80×10^5	178.0259, 149.0594, 134.0363	antioxidant [26]
15	9.26	isochlorogenic acid B	$C_{25}H_{23}O_{12}^-$	515.118	515.1195	2.9119	5.15×10^5	353.0874, 191.0554, 173.0446, 135.0441	*anti*-virus [27]
16	9.34	luteolin 7-*O*-β-D-glucuronide	$C_{21}H_{17}O_{12}^-$	461.0703	461.0725	4.7715	2.33×10^6	285.0399, 151.0031, 133.0285	*anti*-virus [28]

Note: The original MS spectra, and identification process were detailed in Suppl. 1–33. The *m/z* value in bold means the diagnostic fragments. The *m/z* values below 50 were also found by the Xcalibur 4.1 software package, despite the fact that the scan mode, the m/z range was set to 100–1500 in the mass spectra. In the square brackets, the m/z value represents the peak of the molecular ion. Nominal level values were obtained by the Xcalibur 4.1 software package. Three compounds (3, 5, and 33) with "+" in the Molecular ion were identified under the positive ion model. Negative ion models were used to identify all other compounds. The positive ion model was the supplement of negative ion model.

No.	RT min	Name	Molecular ion	Observed *m/z* value	Theoretical *m/z* value	Error (δ ppm)	Nominal level	Characteristic MS/MS fragment peak *m/z*	Bioactive effect
17	9.35	quercetin 3-*O*-β-D-glucuronide	$C_{21}H_{17}O_{13}^-$	477.0670	477.0675	1.0480	1.65×10^6	301.0351, 255.0296, 227.0344, 151.0027	antioxidant [29]
18	9.38	ellagic acid	$C_{14}H_5O_8^-$	300.9988	300.999	0.6645	6.36×10^7	283.9962, 257.0092, 229.0135, 200.0187, 145.0286	antioxidant **[30]**
19	9.51	isoquercitrin	$C_{21}H_{19}O_{12}^-$	463.0885	463.0882	0.6478	2.15×10^5	300.0276, 271.0248, 255.0298, 243.0301, 151.0028, 107.0129	antioxidant, *anti*-virus **[8]**
20	9.82	isochlorogenic acid C	$C_{25}H_{23}O_{12}^-$	515.1197	515.1195	0.3883	2.38×10^6	353.0877, 179.0342, 173.0447 135.0442	antiinflammation [31]
21	9.84	baicalin	$C_{21}H_{17}O_{11}^-$	445.0784	445.0776	1.7974	1.75×10^6	311.0561, 269.0456, 113.0234	*anti*-virus [32]
22	9.86	2'-hydroxydaidzein	$C_{15}H_9O_5^-$	269.0456	269.0455	0.3717	1.38×10^6	241.0516, 225.0553, 181.0653	No report
23	9.9	scutellarin	$C_{21}H_{17}O_{12}^-$	461.0725	461.0727	0.4338	6.40×10^5	285.0399, 267.0293, 241.0501	antioxidant [33]
24	9.9	cosmosiin	$C_{21}H_{19}O_{10}^-$	431.0985	431.0984	0.2320	5.31×10^5	268.0378, 211.0395, 151.0029, 117.0336	neuroprotection [34]
25	9.93	isochlorogenic acid A	$C_{25}H_{23}O_{12}^-$	515.1212	515.1195	3.3002	7.83×10^5	353.0873, 173.0450, 135.0446	antioxidant [35]
26	10.00	astragalin	$C_{21}H_{19}O_{11}^-$	447.093	447.0933	0.6710	7.30×10^6	284.0321, 255.0296, 227.0344, 211.0395, 183.0446	*anti*-virus [32]
27	10.62	viscidulin I	$C_{15}H_9O_7^-$	301.0349	301.0354	1.6609	3.51×10^5	151.0031, 133.0290, 121.0290, 107.0133	enzyme inhibition [36]
28	10.86	tiliroside	$C_{30}H_{25}O_{13}^-$	593.1295	593.1301	1.0116	3.18×10^6	447.0927, 285.0399, 255.0293, 227.0344	cytoprotection [37]
29	11.26	kaempferol	$C_{15}H_9O_6^-$	285.0406	285.0405	0.3508	6.80×10^5	255.0300, 229.0506, 108.0207, 93.0340	anti-virus [38]
30	11.38	apigenin	$C_{15}H_9O_5^-$	269.0454	269.0455	0.3717	1.16×10^6	225.0553, 181.0647, 151.0027, 117.0335	anti-virus [38]

Note: The original MS spectra, and identification process were detailed in Suppl. 1–33. The *m/z* value in bold means the diagnostic fragments. The *m/z* values below 50 were also found by the Xcalibur 4.1 software package, despite the fact that the scan mode, the m/z range was set to 100–1500 in the mass spectra. In the square brackets, the m/z value represents the peak of the molecular ion. Nominal level values were obtained by the Xcalibur 4.1 software package. Three compounds (3, 5, and 33) with "+" in the Molecular ion were identified under the positive ion model. Negative ion models were used to identify all other compounds. The positive ion model was the supplement of negative ion model.

No.	RT min	Name	Molecular ion	Observed *m/z* value	Theoretical *m/z* value	Error (δ ppm)	Nominal level	Characteristic MS/MS fragment peak *m/z*	Bioactive effect
31	12.8	6-gingerol	$C_{17}H_{25}O_4^-$	293.1752	293.1758	2.0466	2.97×10^6	236.1050, 221.1541, 205.1229, 148.0520	antioxidant [39]
32	16.16	ethyl stearate	$C_{20}H_{39}O_2^-$	311.2956	311.2956	0	8.32×10^4	133.0653, 119.0497	neurodevelopment [40]
33	16.79	(+)-4-cholesten-3-one	$C_{27}H_{45}O^+$	385.3456	385.3465	2.3356	2.28×10^5	367.3353, 123.0804, 109.0650	antitumor [41]

Note: The original MS spectra, and identification process were detailed in Suppl. 1–33. The *m/z* value in bold means the diagnostic fragments. The *m/z* values below 50 were also found by the Xcalibur 4.1 software package, despite the fact that the scan mode, the m/z range was set to 100–1500 in the mass spectra. In the square brackets, the m/z value represents the peak of the molecular ion. Nominal level values were obtained by the Xcalibur 4.1 software package. Three compounds (3, 5, and 33) with "+" in the Molecular ion were identified under the positive ion model. Negative ion models were used to identify all other compounds. The positive ion model was the supplement of negative ion model.

As seen in Suppls. 1–33, all identified compounds have been fully elucidated for their MS spectra fragmenting. These fragmenting pathways adhered to classical MS spectra principles, such as *retro* Diels-Alder fragmenting [42]. The full elucidation of isoquercitrin was a good example, through which the *δ* values were found to vary from 0.0 ppm to 3.9 ppm (Fig. 5). So low *δ* values have witnessed the high reliability of our putative identification. Similar high reliabilities could also be observed in other MS spectra fragmenting elucidations (Suppls. 1–33).

More importantly, our putative identification has successfully discriminated isomers, e.g., luteolin 7-*O*-β-glucuronide (**16**) and scutellarin (**23**). Both of them showed a strong base peak *m/z* 285 and a weak molecular ion peak *m/z* 461, resulting in highly similar MS/MS profiles. Nevertheless, our new method has effectively distinguished between these two isomers [43]. Furthermore, three mono-caffeoylquinic acid isomers (i.e., **6, 9**, and **11**) have also been strictly discriminated. Similarly, three dicaffeoylquinic acid isomers (i.e., **15, 20**, and **26**) have been clearly discriminated as well (Figs. 3–4 and Suppls. 5, 20, and 26).

The discrimination of isomers, together with the aforementioned full MS spectra elucidation, became our obvious advantage over other UHPLC-Q-Exactive-Orbitrap-MS/MS analyses, such as Wu's analysis. The analysis did not fully elucidate MS spectra; consequently, it did not discriminated isomers and not drawn the stereo-configuration of chiral atoms [44]. Similar limitations were also found in the newest analyses by Song's team [45] and Liu's team [46]. Liu's anaysis has identifed a compound named "4-*O*-dicaffeoylquinic acid". Undoubtedly, this erroneous was far inferior to our strict discriminations invovling mono-caffeoylquinic acid isomers and dicaffeoylquinic acid isomers. These advantages further suggested the high-reliability of our database-affinity UHPLC-Q-Exactive-orbitrap-MS/MS putative identification. This has offered a premise for the biogenetic relationship analysis of 33 compounds.

As seen in Fig. 4, the leaves of *R. alceifolius* contained 12 flavonoids; however, most of them showed certain biogenetic relationships. Tiliroside (**28**), for example, is an acylation product of astragalin (**26**) by cis-4-hydroxycinnamic acid. The acylation could be catalyzed by acyltransferases [47]. Alternatively, astragalin and *cis*-4-hydroxycinnamic acid were formed from the hydrolysis of β-glucosidase and other enzymes [48]. Nevertheless, the co-existence of **13, 26**, and **28** has clearly suggested that there was a biogenetic relationship among them. Other biogenetic relationships were also illustrated in Fig. 4, including glycosidation, hydroxylation, hydroxyccinnamoylation, oxidization, and dimerization. These prevalent biogenetic relationships might further suggest that these identified compounds were host compounds, rather than invasive or guest substances, that drive the growth of plants. When combined with their bioactive effects (Table 1 right column), it can be further inferred that these identified compounds are likely to be important components of *R. alceifolius* leaves used in traditional medicine.

4. Conclusions

In this study a novel database-affinity UHPLC-Q-Exactive-Orbitrap-MS/MS analytical approach is utilized and putatively identified 33 compounds from *Rubus alceifolius* leaves for the first time. Notably, twelve isomeric compounds have been clearly distinguished from one another, and some biogenetic relationships have been found among these compounds. These new findings contribute to the scientific community's understanding of the chemistry of this medicinal plant.

Declarations

Ethics approval and consent to participate

Not applicable.

Competing interests

The authors declare that they have no competing interests.

Funding

This research was funded by the National Nature Science Foundation of China (82374485) and the Science and Technology Project of Education Department of Guangdong Province (Stem Cell Regulation by Active Molecules from Traditional Chinese Medicines).

Authors' contributions

XL contributed to the project design and paper writing. JZ and RC contributed to chemical analysis methodology. SC, CL, NJ, and TC contributed to extraction and analysis experiments. XHL and JZ contributed to data analyses. XL, XHL, SK contributed to paper revision. All authors read and approved the final manuscript.

Acknowledgements

We are grateful for the permission to collect 10 g *R. alceifolius* leaves from Yaowang Hill preservation garden by the Office of Medicinal-plant Outdoor-teaching Base, Guangzhou University of Chinese Medicine.

Availability of data and material

All the data used to support the findings of this study are available from the corresponding author upon reasonable request.

References

1. Royal-botanic-gardens (2023) Plants of the world online. https://powo.science.kew.org/,
2. Baret S,Nicolini E,Le Bourgeois T,Strasberg D (2003) Developmental patterns of the invasive bramble (Rubus alceifolius poiret, rosaceae) in Reunion island: an architectural and morphometric analysis. Ann Bot 91: 39-48.
3. George B P, & Abrahamse, H. (2021) Traditional Uses and Bioactivities of Common Rubus Species With Reference to Cancer: A Mini-Review. Phytopharmaceuticals. Phytopharmaceuticals: Potential Therapeutic Applications, 259-270.
4. Bhuyan B, & Dutta, A. (2021) A review on the phytochemical, pharmacological and traditional profile on the rubus genus in north-eastern and western parts of india. Current Trends in Pharmaceutical Research 8: 1.
5. Lin J,Zhao J,Li T,Zhou J,Hu J,Hong Z (2011) Hepatoprotection in a Rat Model of Acute Liver Damage Through Inhibition of CY2E1 Activity by Total Alkaloids Extracted From Rubus alceifolius Poir. Int J Toxicol 30: 237-243.
6. Clarivate (2023) Clarivate database. http://www.webofknowledge.com 1: 1.
7. Liu S,Li X,Cai R,Chen B,Zeng J,Li C, et al. (2023) UHPLC-Quadrupole-Exactive-Orbitrap-MS/MS-based Putative Identification for Eucommiae Folium (Duzhongye) and its Quality-marker Candidate for Pharmacopeia. J Sep Sci 46: 00.
8. Zeng J,Li X,Cai R,Li C,Chen S (2023) Jinhua Qinggan Granule UHPLC-Q-extractive-Orbitrap-MS assay: Putative identification of 45 potential anti-Covid-19 constituents, confidential addition, and pharmacopoeia quality-markers recommendation. J Food Drug Anal doi.org/10.38212/2224-6614.3466:
9. Chen S,Li X,Zeng J,Cai R,Li C,Chen C B (2023) Library-based UHPLC-Q-Exactive-Orbitrap-MS Putative Identification of Isomeric and Non-isomeric Bioactives from Zibushengfa Tablet and Pharmacopoeia Quality-marker Chemistry. J Liq Chromatogr Relat Technol, 10.1080/10826076.2023.2223640
10. Li X C (2013) Solvent effects and improvements in the deoxyribose degradation assay for hydroxyl radical-scavenging. Food Chem. 141: 2083-2088.
11. Jiang Q,Li X C,Tian Y G,Lin Q Q,Xie H,Lu W B, et al. (2017) Lyophilized aqueous extracts of Mori Fructus and Mori Ramulus protect Mesenchymal stem cells from *OH-treated damage: bioassay and antioxidant mechanism. BMC Complement. Altern. Med. 16: 423.
12. Li X C,Wang T T,Liu J J,Liu Y L,Zhang J,Lin J, et al. (2020) Effect and mechanism of wedelolactone as antioxidant-coumestan on •OH-treated mesenchymal stem cells. Arab. J. Chem. 13 184-192.
13. Cai R,Li X,Li C,Zhu J,Zeng J,Li J, et al. (2022) Standards-Based UPLC-Q-Exactive Orbitrap MS Systematically Identifies 36 Bioactive Compounds in Ampelopsis grossedentata (Vine Tea). Separations 9: 329.
14. Li X C,Chen S M,Zeng J Y,Cai R X,Liang Y L,Chen C B, et al. (2023) Database-aided UHPLC-Q-orbitrap MS/MS Strategy Putatively Identifies 52 Compounds from Wushicha Granule to Propose Anti-counterfeiting Quality-markers for Pharmacopoeia. Chin Med 18:

15. Arumugam M,Paal M,Donohue T J,Ganesan M,Osna N,Kharbanda K (2023) Beneficial Effects of Betaine: A Comprehensive Review. Biology (Basel) 10: 456.
16. Xie H,Li X C,Ren Z X,Qiu W M,Chen J L,Jiang Q, et al. (2018) Antioxidant and Cytoprotective Effects of Tibetan Tea and Its Phenolic Components. Molecules 23: 179.
17. Li J,Wang S P,Wang Y Q,Shi L,Zhang Z K,Dong F, et al. (2021) Comparative metabolism study on chlorogenic acid, cryptochlorogenic acid and neochlorogenic acid using UHPLC-Q-TOF MS coupled with network pharmacology. Chin J Nat Med 19: 212-224.
18. Li X C (2017) 2-Phenyl-4,4,5,5-tetramethylimidazoline-1-oxyl 3-oxide (PTIO•) Radical Scavenging: A New and Simple Antioxidant Assay *In Vitro*. J Agric Food Chem 65: 6288-6297.
19. Liang H,Huang Q,Zou L,Wei P,Lu J,Zhang Y (2023) Methyl gallate: Review of pharmacological activity. Pharmaco Res 194: 106849.
20. Li X C (2012) Improved pyrogallol autoxidation method: a reliable and cheap superoxide-scavenging assay suitable for all antioxidants. J. Agric. Food Chem. 60: 6418-6424.
21. Li X C,Hu Q P,Jiang S X,Li F,Lin J,Han L, et al. (2015) Flos Chrysanthemi Indici protects against hydroxyl-induced damages to DNA and MSCs via antioxidant mechanism. J. Saudi Chem. Soc. 19: 454-460.
22. Mai W,Chen D,Li X J T U o M S (2012) Antioxidant Activity of Rhizoma Cibotii in vitro.
23. Ma X P,Okyere S K,Hu L W,Wen J,Ren Z H,Deng J L, et al. (2022) Anti-Inflammatory Activity and Mechanism of Cryptochlorogenic Acid from Ageratina adenophora. Nutrients 14: 3.
24. Yang H,Xue X,Li H,Apandi S N,Tay-Chan S C,Ong S P, et al. (2018) The relative antioxidant activity and steric structure of green tea catechins - A kinetic approach. Food Chem 257: 399-405.
25. Leon-Carmona J R,Alvarez-Idaboy J R,Galano A (2012) On the peroxyl scavenging activity of hydroxycinnamic acid derivatives: mechanisms, kinetics, and importance of the acid-base equilibrium. Phys. Chem. Chem. Phys. 14: 12534-12543.
26. Amic A,Markovic Z,Dimitric Markovic J M,Milenkovic D,Stepanic V (2019) Antioxidative potential of ferulic acid phenoxyl radical. Phytochemistry 170: 112218.
27. Wu Y,Hao B,Cao H,Xu W,Li Y,Li L (2012) Anti-hepatitis B virus effect and possible mechanism of action of 3,4-o-dicaffeoylquinic Acid in vitro and in vivo. Evid Based Complement Alternat Med 2012: 356806.
28. Mohapatra P K,Chopdar K S,Dash G C,Mohanty A K,Raval M K (2021) In silico screening and covalent binding of phytochemicals of Ocimum sanctum against SARS-CoV-2 (COVID 19) main protease. J. Biomol. Struct. Dyn., 10.1080/07391102.2021.20071701-10.
29. Wu Y B,Zheng L J,Wu J G,Chen T Q,Yi J,Wu J Z (2012) Antioxidant activities of extract and fractions from receptaculum nelumbinis and related flavonol glycosides. Int J Mol Sci 13: 7163-7173.
30. Li X,Chen B,Zhao X,Chen D (2018) 2-Phenyl-4,4,5,5-tetramethylimidazoline-1-oxyl 3-oxide Radical (PTIO•) Trapping Activity and Mechanisms of 16 Phenolic Xanthones. Molecules 23: 1692.
31. Jang G,Lee S,Hong J,Park B,Kim D,Kim C D (2021) Anti-Inflammatory Effect of 4,5-Dicaffeoylquinic Acid on RAW264.7 Cells and a Rat Model of Inflammation. Nutrients 13: 3537.
32. Rakshit G,Dagur P,Satpathy S,Patra A,Jain A,Ghosh M (2022) Flavonoids as potential therapeutics against novel coronavirus disease-2019 (nCOVID-19). J. Biomol. Struct. Dyn. 40: 6989-7001.
33. Liu Q,Li X,Ouyang X,Chen D (2018) Dual Effect of Glucuronidation of a Pyrogallol-Type Phytophenol Antioxidant: A Comparison between Scutellarein and Scutellarin. Molecules 23: 3225.
34. Min Z,Tang Y,Hu X,Zhu B,Ma Y,Zha J, et al. (2018) Cosmosiin Increases ADAM10 Expression via Mechanisms Involving 5'UTR and PI3K Signaling. Front Mol Neurosci 11: 198.
35. Zhang D,Hamdoun S,Chen R,Yang L,Ip C K,Qu Y, et al. (2021) Identification of natural compounds as SARS-CoV-2 entry inhibitors by molecular docking-based virtual screening with bio-layer interferometry. Pharmacol. Res. 172: 105820.
36. Wang L,Tan N,Wang H,Hu J,Diwu W,Wang X (2020) A systematic analysis of natural α-glucosidase inhibitors from flavonoids of Radix scutellariae using ultrafiltration UPLC-TripleTOF-MS/MS and network pharmacology. BMC Complement Med Ther 20: 72.
37. Li X,Tian Y,Wang T,Lin Q,Feng X,Jiang Q, et al. (2017) Role of the p-Coumaroyl Moiety in the Antioxidant and Cytoprotective Effects of Flavonoid Glycosides: Comparison of Astragalin and Tiliroside. Molecules 22: 1165.
38. Luo E,Zhang D,Luo H,Liu B,Zhao K,Zhao Y, et al. (2020) Treatment efficacy analysis of traditional Chinese medicine for novel coronavirus pneumonia (COVID-19): an empirical study from Wuhan, Hubei Province, China. Chin. Med. 15: 34.
39. Lin J,Li X C,Chen L,Lu W Z,Chen X W,Han L, et al. (2014) Protective effect against hydroxyl radical-induced DNA damage and antioxidant mechanism of [6]-gingerol: A Chemical Study. B. Korean Chem. Soc. 35: 1633-1638.
40. Huang J,Yi L,Yang X,Zheng Q,Zhong J,Ye S, et al. (2023) Neural stem cells transplantation combined with ethyl stearate improve PD rats motor behavior by promoting NSCs migration and differentiation. CNS Neurosci Thera, 10.1111/cns.14119

41. Elia J,Carbonnelle D,Logé C,Ory L,Huvelin J,Tannoury M, et al. (2019) 4-cholesten-3-one decreases breast cancer cell viability and alters membrane raft-localized EGFR expression by reducing lipogenesis and enhancing LXR-dependent cholesterol transporters. Lipids Health Dis 18: 168.
42. Hua Y,Li X C,Zhang W,Chen B,Liu Y,Zhao X, et al. (2021) Antioxidant product analysis of Folium Hibisci Mutabilis. J Saudi Chem 25: 101272.
43. Li X C,Zeng J,Cai R,Li C (2023) New UHPLC-Q-Orbitrap MS/MS-based Library-comparison Method Simultaneously Distinguishes 22 Phytophenol Isomers from Desmodium styracifolium. Microchem J 190: 108938.
44. Wu J,Cai B,Zhang A,Zhao P,Du Y,Liu X, et al. (2022) Chemical Identification and Antioxidant Screening of Bufei Yishen Formula using an Offline DPPH Ultrahigh-Performance Liquid Chromatography Q-Extractive Orbitrap MS/MS. Int J Anal Chem 2022: 1423801.
45. Song S,Zhou H,Lan X,Yuan X,Li Y,Huang S, et al. (2023) Comprehensive characterization of narirutin metabolites in vitro and in vivo based on Analogous-Core recursion analysis strategy using UHPLC-Q-Exactive Orbitrap MS/MS. Arab J Chem 16: 104949.
46. Liu T,Cao X,Cao D (2022) Combination of UHPLC-Q Exactive-Orbitrap MS and network pharmacology to reveal the mechanism of Eucommia ulmoides leaves in the treatment of osteoarthritis. J Food Biochem 46: e14204.
47. Aktar S,Bai P,Wang L,Xun H,Zhang R,Wu L, et al. (2023) Identification of a BAHD Acyltransferase Gene Involved in Plant Growth and Secondary Metabolism in Tea Plants. Plants (Basel) 11: 2483.
48. Karami F,Ghorbani M,Alireza Sadeghi Mahoonak A S,Pourhossein A,Bagheri A,Khodarahmi R (2022) Increasing Antioxidant Activity in Food Waste Extracts by β-Glucosidase. Food Technol Biotechnol 60: 458-468.

Figures

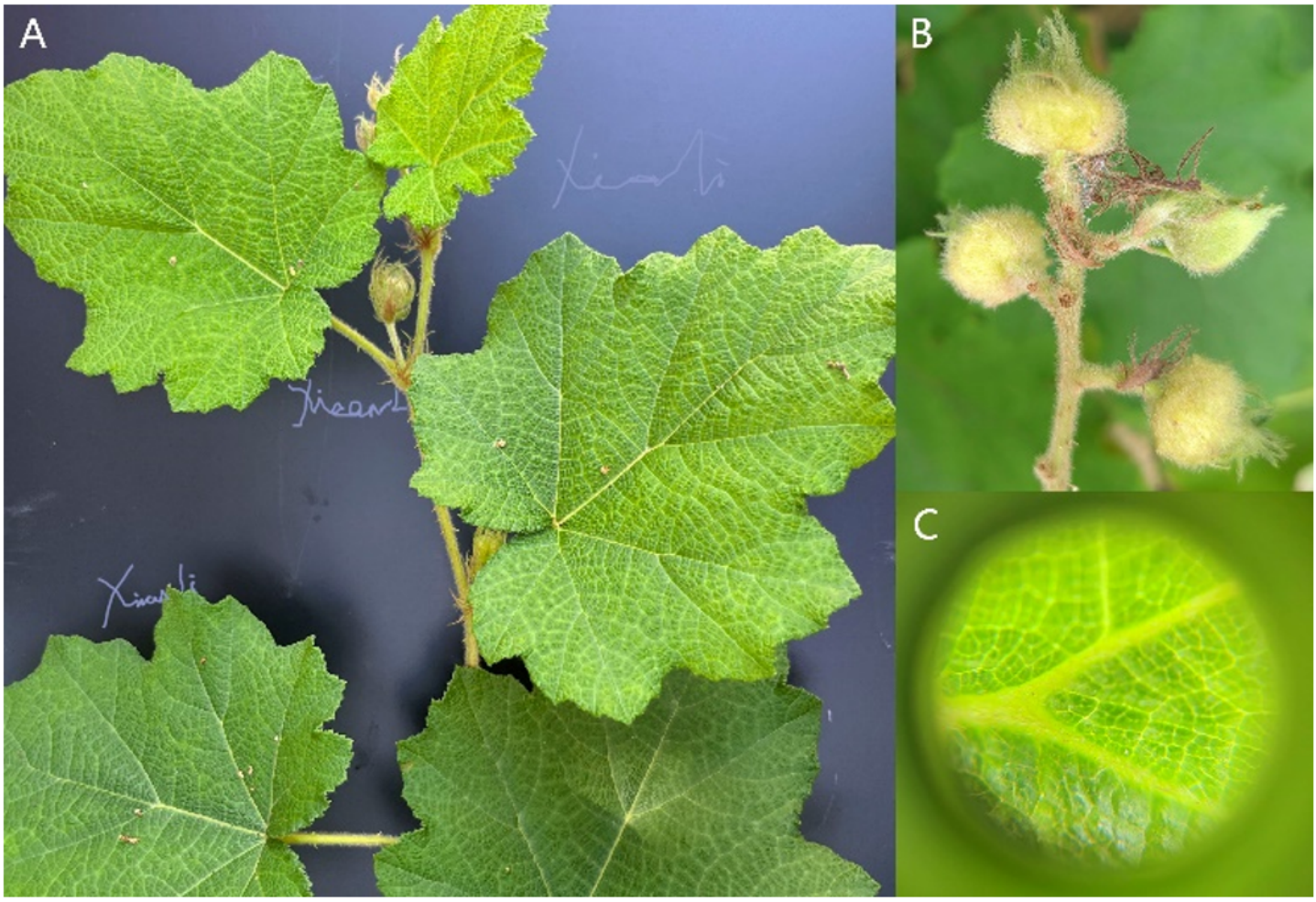

Figure 1

Photos of *R. alceifolius* Poir. A, for its leaves; B, for its fruit; C, for its leaf vein (micrograph view, 40×)

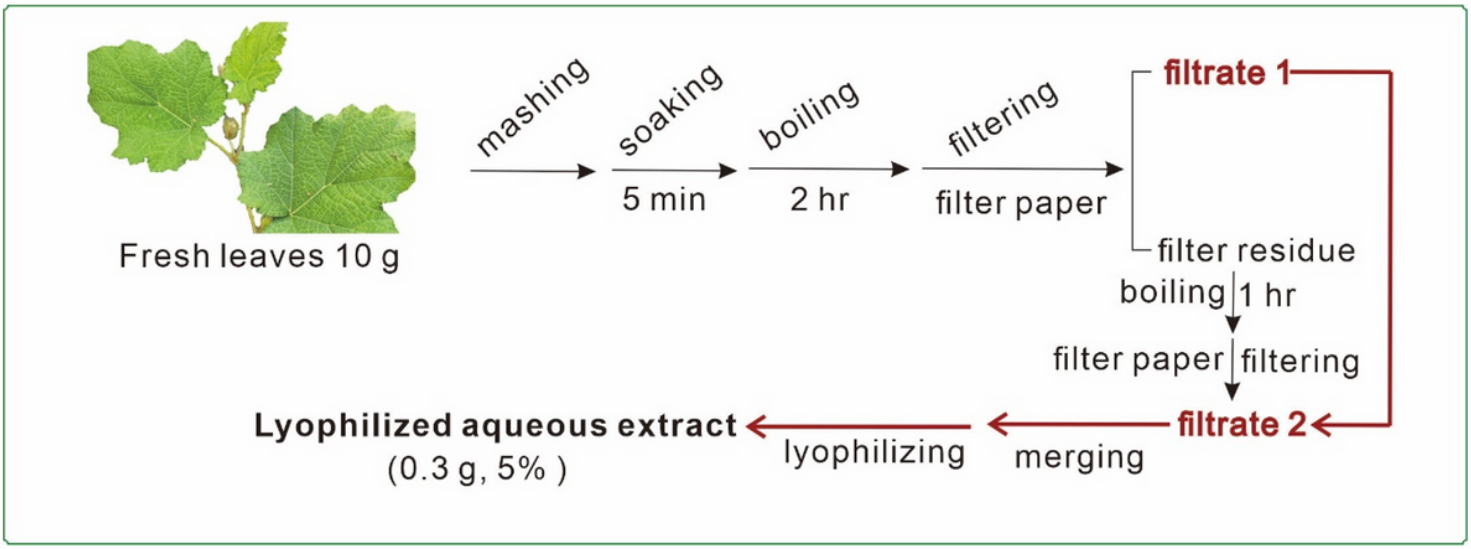

Figure 2

Flow chart of preparation of lyophilized aqueous extract from *R. alceifolius* leaves

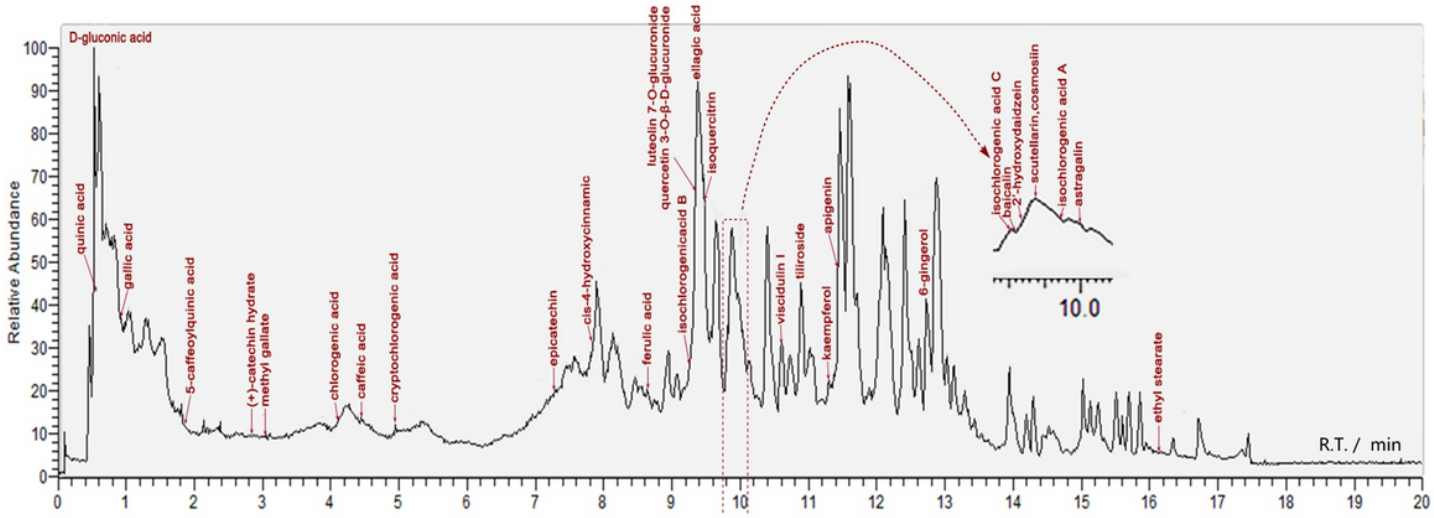

Figure 3

The total ion current (TIC) chromatogram of *R. alceifolius* leaves in the UHPLC-Q-Exactive-orbitrap-MS analysis. (A) The negative ion mode; (B) the positive ion mode. The positive ion mode served as a supplement to the negative ion mode. A positive ion model was symbolized by “a”. Considering the layout space, the TIC diagram under the positive ion model was not shown in the main text.

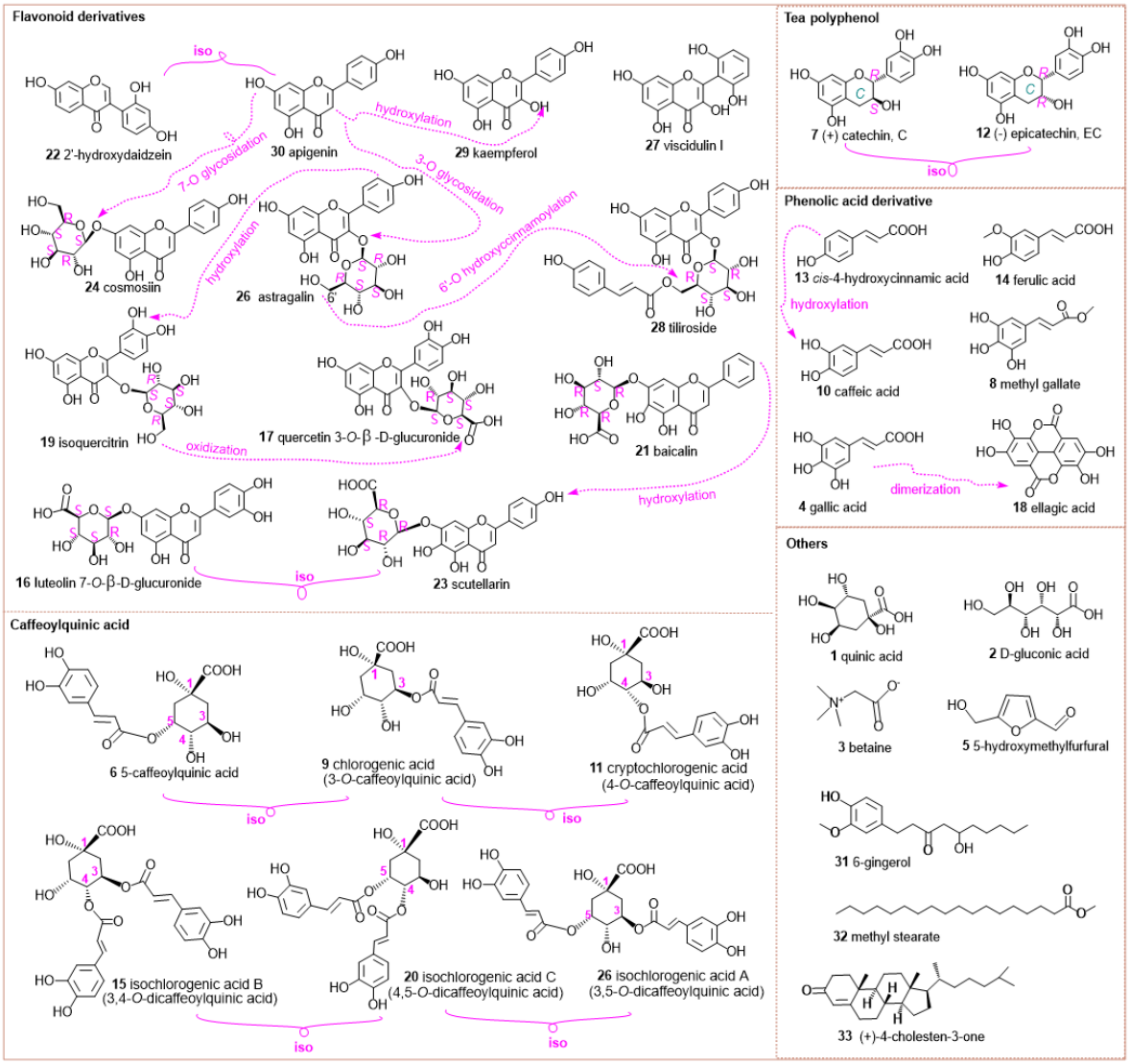

Figure 4

The structures, configurations, and biogenetic relationship of 33 identified compounds. Knot line with "*iso*" connected two isomers.

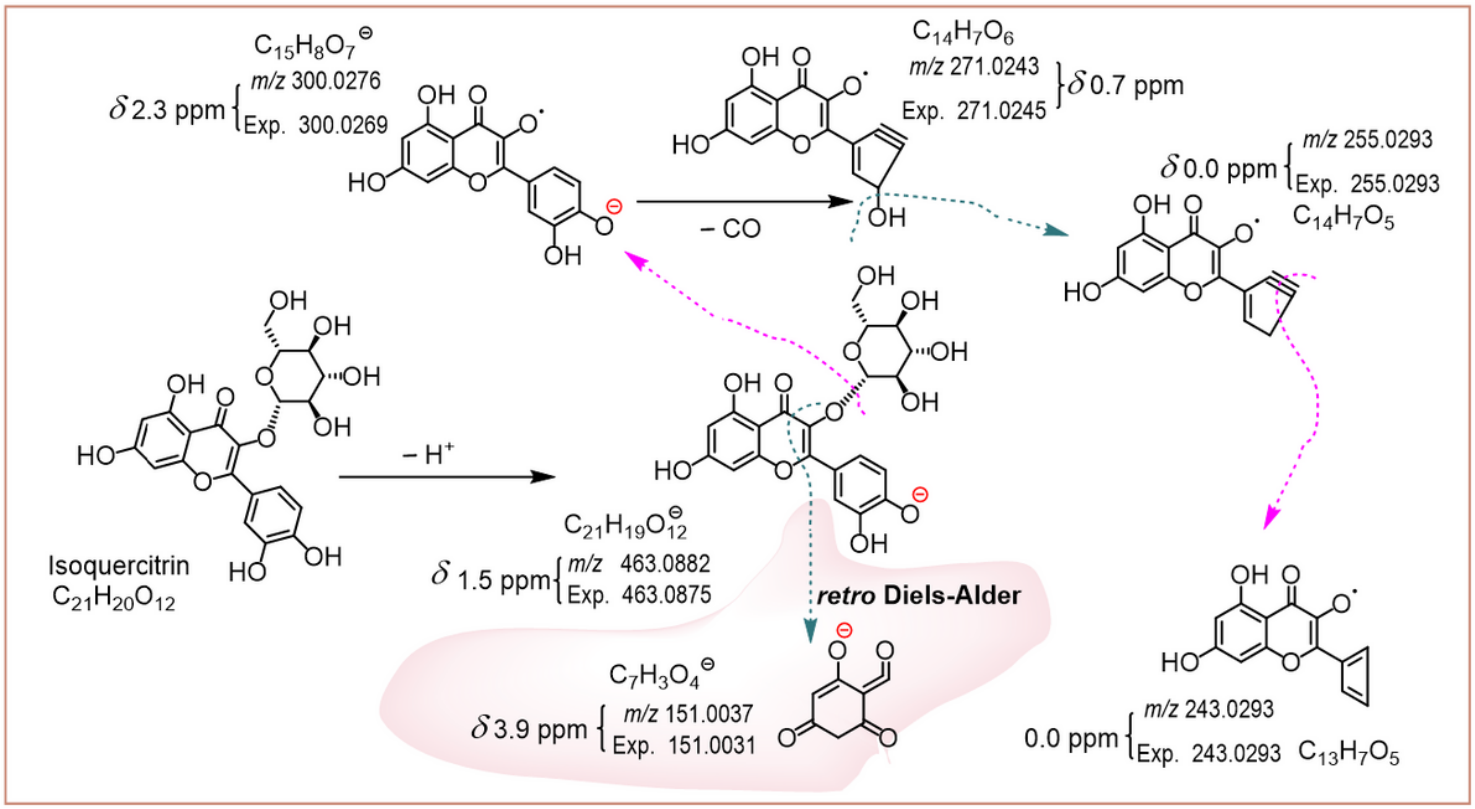

Figure 5

Typical fragmenting pathways comprising *retro*Diels-Alder of flavonoid (isoquercitrin as example)

Supplementary Files

This is a list of supplementary files associated with this preprint. Click to download.

- Suppl1.QuinicacidCAS77952.docx
- Suppl10.CaffeicacidCAS331395.docx
- Suppl11.CryptochlorogenicacidCAS905997.docx
- Suppl12.EpicatechinCAS490460.docx
- Suppl13.Cis4HydroxycinnamicAcidCAS4501319.docx
- Suppl14.FerulicacidCAS1135246.docx
- Suppl15.IsochlorogenicacidBCAS14534613.docx
- Suppl16.Luteolin7OglucuronideCAS29741104.docx
- Suppl17.Quercetin3ObetaDglucuronideCAS22688795.docx
- Suppl18.EllagicacidCAS476664.docx
- Suppl19.IsoquercitrinCAS21637252.docx
- Suppl2.DgluconicacidCAS526954.docx
- Suppl20.IsochlorogenicacidCCAS57378720.docx
- Suppl21.BaicalinCAS21967419.docx
- Suppl22.2hydroxydaidzeinCAS7678855.docx
- Suppl23.ScutellarinCAS27740018.docx
- Suppl24.cosmosiinCAS578745.docx
- Suppl25.IsochlorogenicacidACAS2450535.docx
- Suppl26.astragalinCAS480104.docx
- Suppl27.ViscidulinICAS92519954.docx

- Suppl28.TilirosideCAS20316625.docx
- Suppl29.KaempferolCAS520183.docx
- Suppl3.BetaineCAS107437.docx
- Suppl30.ApigeninCAS520365.docx
- Suppl31.6gingerolCAS23513146.docx
- Suppl32.EthylStearateCAS111615.docx
- Suppl33.4cholesten3oneCAS601570.docx
- Suppl4.GallicacidCAS149917.docx
- Suppl5.5HydroxymethylfurfuralCAS67470.docx
- Suppl6.5caffeoylquinicacidCAS906332.docx
- Suppl7.CatechinhydrateCAS225937100.docx
- Suppl8.MethylgallateCAS99241.docx
- Suppl9.ChlorogenicAcidCAS327979.docx
- graphabstract.png